Heat Transfer from Parallel Flow Through Isosceles Triangular and Rectangular Tube Bundles

B. T. F. Chung,* F. Liu,† and M. M. Kermani‡
The University of Akron, Akron, Ohio
and
L. T. Yeh§
Texas Instruments Inc., Dallas, Texas

In this work, the Nusselt number and the heat transfer characteristics of the longitudinal flow through isosceles triangular and rectangular rod bundles are studied analytically. The flow under consideration is steady, laminar, and fully developed both thermally and hydrodynamically, and the thermophysical properties are constant. Two different boundary conditions are included. They are 1) uniform heat flux along axial direction and uniform wall temperature along circumferential direction and 2) uniform wall heat flux along both axial and circumferential directions.

Nomenclature

$A,B,\ldots,E$ = constants in temperature solutions
C_p = specific heat
d = diameter of rod, $2r_0$
d_h = hydraulic diameter
h = heat transfer coefficient
(H_1) = uniform wall temperature boundary condition circumferentially
(H_2) = uniform wall heat flux boundary condition circumferentially
j = summation index
k = conductivity
n = direction of the normal
Nu_d = Nusselt number based on rod diameter, hd/k
Nu_{dh} = Nusselt number based on hydraulic diameter, $h(d_h)/k$
p = static pressure
Q = heat transfer rate per unit length of one-half cylinder
q, q_W = local wall heat transfer rate per unit area, $-k\left.\frac{\partial T}{\partial r}\right|_{r=r_0}$
$\bar{q}$ = circumferential average of heat flux, $Q/\pi r_0$
r = radial coordinate
$\bar{r}$ = dimensionless radial coordinate $r/(s_3/2)$
r_0 = radius of rod
$\bar{r}_0$ = dimensionless radius of rod $r_0/(s_3/2)$
$\bar{r}_1$ = dimensionless radial distance defined in Fig. 2a
r^* = distance defined by Eq. (12)
s = s_2/s_3
s_2 = spacing between centers of two adjacent cylinders in x direction
s_3 = spacing between centers of two cylinders in y direction defined in Figs. 1a and 1b
T = temperature
$\bar{T}$ = dimensionless temperature, $(T-T_{WO})/(Q/kW)$
T_{WO} = average wall temperature
u = axial velocity
$\bar{u}$ = dimensionless velocity, $u\Big/\left[-\frac{1}{\mu}\frac{dp}{dz}\left(\frac{s_3}{2}\right)^2\right]$
W = volume flow rate in one-half cylinder
$\bar{W}$ = $W\Big/\left[-\frac{1}{\mu}\frac{dp}{dz}\left(\frac{s_3}{2}\right)^4\right]$
z = axial coordinate measuring distance from the entrance to the passage
θ = angular coordinates shown in Fig. 2
θ_0 = angle between center-to-center connecting lines
δ = $\delta=1$ for triangular, $\delta=0.5$ for rectangular arrays
μ = dynamic viscosity
ρ = density of fluid
ϵ = porosity, $1-\pi r_0^2/2s$

Introduction

HEAT transfer to a laminar flow from arrays of parallel rods or tubes has significant application in the design of compact heat exchangers and nuclear reactors Consequently, extensive studies in both experimental[1-7] and theoretical[8-15] aspects of this field have been reported in the literature. Excellent and comprehensive reviews on longitudinal flow and heat transfer for the rod bundle geometry have been presented by Axford[16] and Shah and London.[17] However, all theoretical heat transfer solutions obtained to date by the aforementioned authors are restricted to the geometry of either delta (equilateral triangle) or square arrays. The present analysis is concerned with more general configurations, namely, isosceles triangular and rectangular arrays. The former includes the equilateral triangular arrangement as its limiting case, whereas the latter includes the square array configuration as its limiting case. In this connection, the present authors have just completed a study on the velocity distribution of the longitudinal flow through isosceles triangular and rectangular rod bundles.[18] The general expression for the velocity distribution is employed in the present heat transfer analysis.

The purpose of this work is to determine the heat transfer characteristics and Nusselt number of the longitudinal flow through isosceles triangular and rectangular rod bundles. The schematic diagrams of the situation under this study are

Presented as Paper 87-0079 at the AIAA 25th Aerospace Sciences Meeting, Reno, NV, Jan. 12-15, 1987; received Feb. 6, 1987; revision received June 5, 1987.

*Professor, Department of Mechanical Engineering.
†Research Associate, Department of Mechanical Engineering. Formerly Visiting Scientist from Chinese Academy of Space Technology.
‡Graduate Assistant, Department of Mechanical Engineering.
§Senior Engineer.

shown in Figs. 1a and 1b that represent the axial flow in isosceles triangular array and rectangular array, respectively. In the present analysis, it is assumed that the flow is steady, laminar, and fully developed both thermally and hydrodynamically; the thermophysical properties are constant. A uniform heat flux is applied along the axial direction; two different boundary conditions are considered in the circumferential direction, namely, uniform heat flux and uniform wall temperature.

Analysis

To analyze the heat transfer of the system, we merely consider the representative shaded areas bounded by *ABCD* in Fig. 1a or *AQON* in Fig. 1b. Note that the flow is symmetrical with respect to the origin 0 and two axes *MN* and *PQ* in Fig. 1b, but is symmetrical with respect to the origin only in Fig. 1a. The governing equation of the system can be conveniently expressed in cylindrical coordinates as follows:

$$\rho C_p u \frac{\partial T}{\partial z} = k\left(\frac{\partial^2 T}{\partial r^2} + \frac{1}{r}\frac{\partial T}{\partial r} + \frac{1}{r^2}\frac{\partial^2 T}{\partial \theta^2} + \frac{\partial^2 T}{\partial z^2}\right) \quad (1)$$

Let Q be the heat flux per unit length along the axial direction. From energy balance

$$Q = \rho C_p W \frac{\partial T}{\partial z} = \text{const}$$

which gives

$$\frac{\partial^2 T}{\partial z^2} = 0 \quad \text{and} \quad T = \frac{Q}{\rho C_p W} z + T(r,\theta)$$

for constant thermal properties. If we utilize the foregoing relationship, Eq. (1) can be rewritten in the following nondimensional form:

$$\bar{u} = \frac{\partial^2 \bar{T}}{\partial \bar{r}^2} + \frac{1}{\bar{r}}\frac{\partial \bar{T}}{\partial \bar{r}} + \frac{1}{\bar{r}^2}\frac{\partial^2 \bar{T}}{\partial \theta^2} \quad (2)$$

In the aforementioned expressions, $\bar{u}$ is the axial velocity as functions of r and θ and is obtained from the solution of momentum equation of the same system.[18] The pertaining boundary conditions of Eq. (2) are depicted in Figs. 2a and 2b, respectively. In both, the dimensions are normalized by $s_3/2$ and also n denotes the normal direction to a specific boundary. The conditions along the boundaries 1 to 6 shown in Fig. 2 can be mathematically described as follows.

1) Uniform wall heat flux axially and uniform wall temperature circumferentially, (H1)

$$① \frac{\partial \bar{T}}{\partial n} = \frac{\partial \bar{T}}{\partial \theta} = 0 \quad \text{at} \quad \theta = \frac{\pi}{2} \quad (3)$$

$$② \bar{T} = 0 \quad \text{at} \quad \bar{r} = \bar{r}_0 \quad (4)$$

$$③ \frac{\partial \bar{T}}{\partial n} = \frac{\partial \bar{T}}{\partial \theta} = 0 \quad \text{at} \quad \theta = 0 \quad (5)$$

$$④ \frac{\partial \bar{T}}{\partial \bar{r}}\cos\theta - \frac{1}{\bar{r}}\frac{\partial \bar{T}}{\partial \theta}\sin\theta = 0$$

$$\text{at} \quad \bar{r} = \frac{s}{\cos\theta}, \quad 0 \le \theta \le \arctan\frac{1-\bar{r}_0}{s} \quad (6)$$

$$④' \frac{\partial \bar{T}}{\partial \bar{r}}\cos\theta - \frac{1}{\bar{r}}\frac{\partial \bar{T}}{\partial \theta}\sin\theta = 0$$

$$\text{at} \quad \bar{r} = \frac{s}{\cos\theta}, \quad 0 \le \theta \le \arctan\frac{1}{2s} \quad (7)$$

$$⑤ \bar{T} = 0 \quad \text{at} \quad \bar{r} = r^*,$$

$$\arctan(1-\bar{r}0)/s \le \theta \le \arctan 1/(s-\bar{r}0) \quad (8)$$

where

$$r^* = s\cos\theta + \sin\theta - \sqrt{\bar{r}_0^2 - (s\sin\theta - \cos\theta)^2}$$

$$⑥ \frac{\partial \bar{T}}{\partial \bar{r}}\sin\theta + \frac{1}{\bar{r}}\frac{\partial \bar{T}}{\partial \theta}\cos\theta = 0$$

$$\text{at} \quad \bar{r} = \csc\theta, \quad \arctan\frac{1}{s-\bar{r}_0} \le \theta \le \frac{\pi}{2} \quad (9)$$

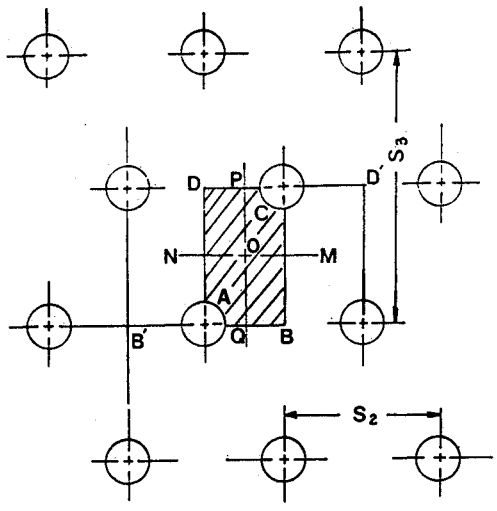

Fig. 1a Schematic diagram of longitudinal flow through isosceles triangular array of rods.

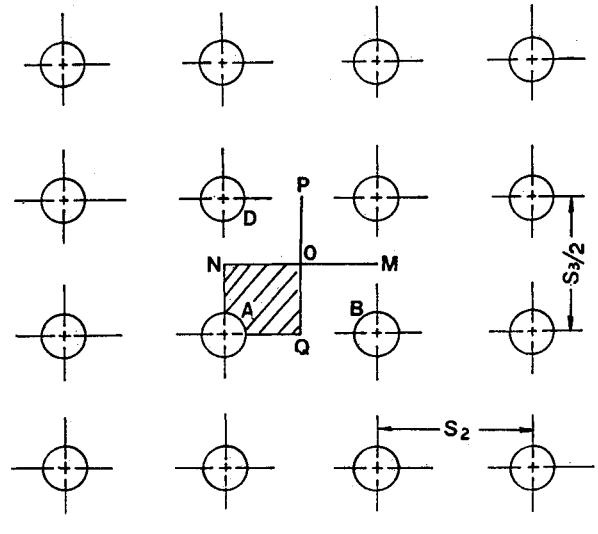

Fig. 1b Schematic diagram of longitudinal flow through rectangular array of rods.

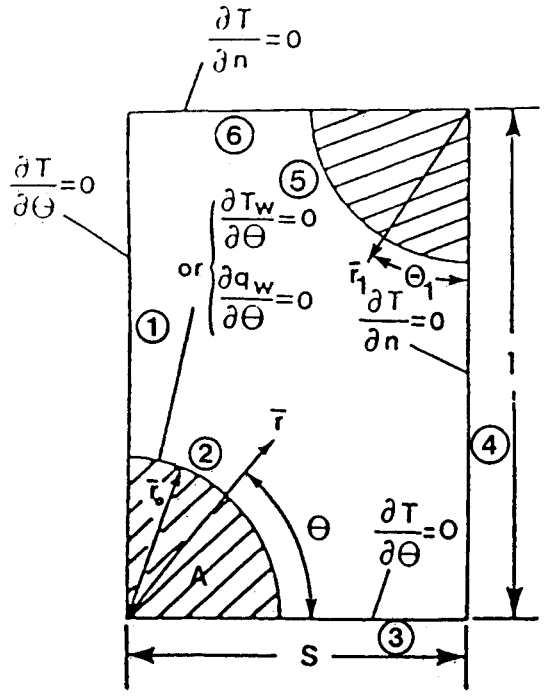

Fig. 2a A typical element of isosceles triangular array with the corresponding boundary conditions.

$$⑥'\quad \frac{\partial \bar{T}}{\partial \bar{r}}\sin\theta+\frac{1}{\bar{r}}\frac{\partial \bar{T}}{\partial \theta}\cos\theta=0$$

$$\text{at}\quad \bar{r}=0.5\csc\theta,\qquad \arctan\frac{1}{2s}\le\theta\le\frac{\pi}{2} \tag{10}$$

2) Uniform wall heat flux axially and circumferentially, ⑫. The conditions ①, ③, ④, ④', ⑥, and ⑥' are the same as in case 1.

$$②\quad -k\frac{\partial T}{\partial r}=\frac{Q}{\pi r_0}=\text{const}\qquad \text{at}\qquad r=r_0$$

that is,

$$\frac{\partial \bar{T}}{\partial \bar{r}}=-\frac{\bar{W}}{\pi \bar{r}_0}\qquad \text{at}\qquad \bar{r}=\bar{r}_0 \tag{11}$$

$$⑤\quad \frac{\partial \bar{T}}{\partial \bar{r}_1}=-\frac{\bar{W}}{\pi \bar{r}_0}\qquad \text{at}\qquad \bar{r}_1=\bar{r}_0$$

Using the following relationship between $(\bar{r},\theta)$ and $(\bar{r}_1,\theta_1)$

$$\bar{r}\sin\theta+\bar{r}_1\cos\theta_1=1$$

$$\bar{r}\cos\theta+\bar{r}_1\sin\theta_1=s$$

and after some algebraic manipulations, one obtains

$$\sin(\theta+\theta_1)\frac{\partial \bar{T}}{\partial \bar{r}}+\frac{1}{\bar{r}}\cos(\theta+\theta_1)\frac{\partial \bar{T}}{\partial \theta}=\frac{W}{\pi \bar{r}_0}$$

$$\text{at}\quad r=r^*,\qquad 0\le\theta_1\le\frac{\pi}{2} \tag{12}$$

where r^* has been defined earlier and θ and θ_1 are related by

$$\theta=\arctan\frac{1-\bar{r}_0\cos\theta_1}{s-\bar{r}_0\sin\theta_1} \tag{13}$$

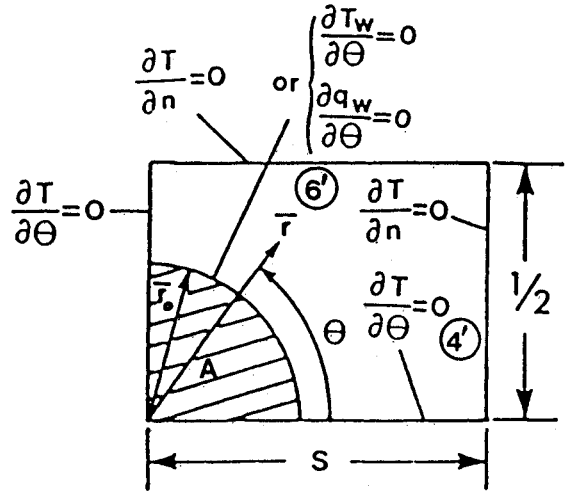

Fig. 2b A typical element of rectangular array with the corresponding boundary conditions.

The velocity distribution in Fig. 2 can be obtained from the solution of the momentum equation and has the form of

$$\bar{u}=\frac{s}{\pi}\ln\frac{\bar{r}}{\bar{r}_0}-\frac{\bar{r}^2-\bar{r}_0^2}{4}+\sum_{j=1}^{\infty}=C_j\bar{r}^{+2j}$$

$$\times\left[1-\left(\frac{\bar{r}_0}{\bar{r}}\right)^{4j}\right]\cos 2j\theta \tag{14}$$

where the Fourier series coefficient C_j was determined from the collocation method.[18] Similarly, the energy equation, Eq. 2, can be solved using the same approach; the complementary solution $\bar{T}_c$ and the particular integral $\bar{T}_p$ of $\bar{T}$ are expressed by

$$\bar{T}_c=(A+B\ln\bar{r})(E_{01}+E_{02}\theta)+\sum_{k=1}^{\infty}(D_{1k}\bar{r}^{\,k}+D_{2k}\bar{r}^{-k})$$

$$\times(E_k\cos k\theta+F_k\sin k\theta) \tag{15}$$

$$\bar{T}_p=\frac{s\bar{r}^{\,2}}{4\pi}\ln\frac{\bar{r}}{\bar{r}_0}-\frac{s\bar{r}^{\,2}}{4\pi}-\frac{\bar{r}^{\,4}-4\bar{r}_0^{\,2}\bar{r}^{\,2}}{64}$$

$$+\sum_{j=1}^{\infty}\frac{C_j}{4}\bar{r}^{\,2j+2}\left[\frac{1}{2j+1}+\frac{1}{2j-1}\left(\frac{\bar{r}_0}{\bar{r}}\right)^{4j}\right]\cos 2j\theta \tag{16}$$

with

$$\bar{T}=\bar{T}_c+\bar{T}_p \tag{17}$$

For the constant heat flux along the axial direction, the following relation holds:

$$-2\int_0^{\pi/2}k\frac{\partial T}{\partial r}\bigg|_{r=r_0}r_0\,d\theta=Q$$

or

$$\int_0^{\pi/2}\frac{\partial \bar{T}}{\partial \bar{r}}\bigg|_{\bar{r}=\bar{r}_0}d\theta=-\frac{\bar{W}}{2\bar{r}_0} \tag{18}$$

Combining Eqs. (3-5) and (15-18) yields the temperature profile of the fluid for uniform tube wall temperature along

the circumferential direction of the form

$$\bar{T}=\left[-\frac{\bar{W}}{\pi}+\frac{S(\bar{r}_0^2+\bar{r}^2)}{4\pi}-\frac{\bar{r}_0^4}{16}\right]\ln\frac{\bar{r}}{\bar{r}_0}-\frac{s(\bar{r}^2-\bar{r}_0^2)}{4\pi}$$
$$-\frac{\bar{r}^4-4\bar{r}_0^2\bar{r}^2+3\bar{r}_0^4}{64}+\frac{1}{4}\sum_{j=1}^{\infty}C_j\bar{r}^{2j+2}\left[\frac{1}{2j+1}\right.$$
$$\left.+\frac{1}{2j-1}\left(\frac{\bar{r}_0}{\bar{r}}\right)^{4j}-\frac{4j}{4j^2-1}\left(\frac{\bar{r}_0}{\bar{r}}\right)^{4j+2}\right]\cos 2j\theta$$
$$+\sum_{j=1}^{\infty}D_j\bar{r}^{2j}\left[1-\left(\frac{\bar{r}_0}{\bar{r}}\right)^{4j}\right]\cos 2j\theta \qquad (19)$$

Similarly, substituting Eqs. (3), (5), (11), and (18) into Eqs. (15–17) gives the temperature profile of the fluid for the case of uniform wall heat flux along the angular direction

$$\bar{T}=\left[-\frac{\bar{W}}{\pi}+\frac{S(\bar{r}_0^2+\bar{r}^2)}{4\pi}-\frac{\bar{r}_0^4}{16}\right]\ln\frac{\bar{r}}{\bar{r}_0}-\frac{s(\bar{r}^2-\bar{r}_0^2)}{4\pi}$$
$$-\frac{\bar{r}^4-4\bar{r}_0^2\bar{r}^2+3\bar{r}_0^4}{64}+\frac{1}{4}\sum_{j=1}^{\infty}C_j\bar{r}^{2j+2}\left[\frac{1}{2j+1}\right.$$
$$\left.+\frac{1}{2j-1}\left(\frac{\bar{r}_0}{\bar{r}}\right)^{4j}+\frac{2}{4j^2-1}\left(\frac{\bar{r}_0}{\bar{r}}\right)^{4j+2}\right]\cos 2j\theta$$
$$+\sum_{j=1}^{\infty}D_j\bar{r}^{2j}\left[1+\left(\frac{\bar{r}_0}{\bar{r}}\right)^{4j}\right]\cos 2j\theta \qquad (20)$$

The collocation method is employed to determine the coefficients Cj's from the appropriate boundary condition of flow[18] and to determine Dj's from Eqs. (6–12). By choosing N points on the boundaries 4 (or 4′), 5, and 6 (or 6′), we will have N terms of the series in Eqs. (19) or (20) that, in turn, yield N linear algebraic equations in terms of D_1, D_2, ..., and D_N. They are then solved simultaneously using standard numerical schemes. Note that Eq. (20) is applicable to any isosceles triangular array and rectangular array [so is Eq. (19)], whereas its counterpart of Eq. (15) of Ref. 8 is only restricted to equilateral triangular array and Eq. (14) of Ref. 15 is limited to square arrays only.

Physically, the first solution is appropriate for the rods with high conductivity and the second solution is applicable to the rods with low conductivity. Once the temperature distribution is obtained, the Nusselt number can be computed from

$$Nu_d=\frac{hd}{k}=\frac{2}{\pi}\frac{\bar{W}}{\bar{T}_{WO}-\bar{T}_b}=-\frac{2}{\pi}\frac{\bar{W}}{\bar{T}_b} \qquad (21)$$

The bulk stream temperature $\bar{T}_b$ is obtained from

$$\bar{T}_b=\int\int_A\bar{T}\bar{u}\bar{r}\,d\bar{r}\,d\theta\Big/\int\int_A\bar{u}\bar{r}\,d\bar{r}\,d\theta \qquad (22)$$

where A denotes the flow area shown in Fig. 2. Coupling Eqs. (25) and (26) yields

$$Nu_d=-\frac{2}{\pi}\left(\bar{W}^2\Big/\int\int_A\bar{T}\bar{u}\bar{r}\,d\bar{r}\,d\theta\right) \qquad (23)$$

The Nusselt number based on the hydraulic diameter can be easily computed from the following relationship:

$$Nu_{dh}=Nu_d\frac{d_h}{d}=Nu_d\left(\frac{4s-2\pi\bar{r}_0^2}{2\pi\bar{r}_0^2}\right)=Nu_d\left(\frac{2s}{\pi\bar{r}_0^2}-1\right) \qquad (24)$$

It is of interest to examine $q/\bar{q}$ for the case of uniform wall temperature around θ and $\bar{T}_W$ for uniform angular wall heat flux condition. They can be obtained from Eqs. (20) and

$$\frac{q}{\bar{q}}=\left(\frac{-k\left.\frac{\partial T}{\partial r}\right|_{r=r_0}}{\frac{Q}{\pi r_0}}\right)$$
$$-\frac{\pi}{\bar{W}}\sum_{j=1}^{\infty}\left(C_j\frac{j}{2j-1}\bar{r}_0^{2j+2}+4D_j j\bar{r}_0^{2j}\right)\cos 2j\theta \qquad (25)$$

and

$$\bar{T}_W=\sum_{j=1}^{\infty}\left(C_j\frac{\bar{r}_0^{2j+2}}{4j-2}+2D_j\bar{r}_0^{2j}\right)\cos 2j\theta \qquad (26)$$

Results and Discussion

To demonstrate the validity and accuracy of the present solutions, we first consider the limiting condition of $\theta=60$ deg, for which Nu_{dh} was tabulated by Dwyer and Berry[9] for both angular boundary conditions of $\partial T_W/\partial\theta=0$ and $\partial q_W/\partial\theta$ and Nu_{dh} was presented in graphical form by Sparrow et al.[8] for the case of $\partial T_W/\partial\theta=0$.

Table 1 shows Nu_{dh} as functions of $s/\bar{r}_0$ at two different circumferential boundary conditions. As can be seen, good agreement is found among all solutions, especially for large values of $s/\bar{r}_0$. However, only the present work extends calculations all the way to $s/\bar{r}_0=1$, i.e., three rods in contact. References 8 and 9 only carried their calculations to $s/\bar{r}_0=1.1$ and 1.001, respectively, due to mathematical difficulties. The former applied the collocation method and the latter used the finite-difference approach directly.

The predicted Nusselt number based on the actual rod diameter Nu_d as a function of porosity ϵ for the isosceles triangular arrays is depicted in Fig. 3. The porosity is defined as the fraction of total cross section available to flow; in terms of Fig. 2, we can write $\epsilon=1-\pi\bar{r}_0^2/2s$. In Fig. 3a, 60 deg $\le\theta_0\le$ 90 deg and 0 deg $\le\theta_0\le$ 30 deg, whereas in Fig. 3b, 30 deg $\le\theta_0\le$ 60 deg where θ_0 is the angle between the center lines of the tubes as shown in the sketch. For the geometry shown in Fig. 3a, the top and bottom rods will never touch but the bottom two rods can be in contact; the opposite statement holds for the case of 30 deg $\le\theta_0\le$ 60 deg. The only situation where three tubes are in contact is when $\theta_0=60$ deg (equilateral triangle). Numerical results of Dwyer and Berry are also included in Fig. 3a. It should be of interest to thermal designers that an optimum heat transfer coefficient exists for all θ_0 under the circumferential boundary condition $\partial q_W/\partial\theta=0$. In the case of $\partial T_W/\partial\theta=0$ (see Fig. 4), the heat transfer rate behaves quite differently, especially at the small ϵ, a significant region for the fuel assemblies in nuclear reactor design. Unlike those in Fig. 3, the curves shown in Fig. 4 do not always have the maximum point. Numerical comparisons of Figs. 3 and 4 reflect that the heat transfer coefficient based on the (H_1) condition always exceeds the counterpart of the (H_2) condition.

On the other hand, the heat transfer coefficient from the laminar parallel flow to rods of rectangular arrays is always less than the counterpart of triangular arrays. This can be seen in Figs. 5 and 6. The trend of the Nusselt number of rectangular array is similar to that of triangular arrays, except that the intersection of a few curves appears in Fig. 6. This phenomenon does not appear in Figs. 4a and 4b.

Table 1 Nusselt numbers Nu_{dh} for equilateral triangular ($\theta_0 = 60$ deg) as functions of $s/\bar{r}_0$ and circumferential boundary conditions

	Uniform wall temperature (H1)		Uniform wall heat flux (H2)		
$s/\bar{r}_0$	Present work	Ref. 9	Ref. 9	Present work	ϵ
1.0	1.198			0.1511	0.0931
1.001	1.225	1.26	0.149	0.1600	0.0949
1.01	1.476	1.52	0.263	0.2532	0.1110
1.02	1.772	1.82	0.404	0.4133	0.1283
1.03	2.086	2.14	0.580	0.5918	0.1452
1.04	2.427	2.48	0.795	0.8077	0.1615
1.05	2.775	2.82	1.06	1.064	0.1774
1.06	3.132	3.18	1.36	1.364	0.1929
1.07	3.493	3.54	1.70	1.705	0.2079
1.10	4.565	4.62	2.92	2.928	0.2505
1.15	6.164			5.135	0.3142
1.20	7.453	7.48	6.90	6.953	0.3702
1.30	9.174	9.19	9.03	9.044	0.4634
1.40	10.311	10.34	10.28	10.287	0.5373
1.50	11.247	11.24	11.22	11.241	0.5969
1.60	12.079	12.08	12.05	12.057	0.6457
1.75	13.269	13.28	13.26	13.264	0.7039
1.80	13.662	13.68	13.66	13.660	0.7201
1.90	14.451	14.47	14.46	14.438	0.7488
2.0	15.252	15.27	15.26	15.252	0.7733
3.0	23.967			23.966	0.8992
4.0	34.137			34.136	0.9433
11.547	154.39			154.39	0.9921

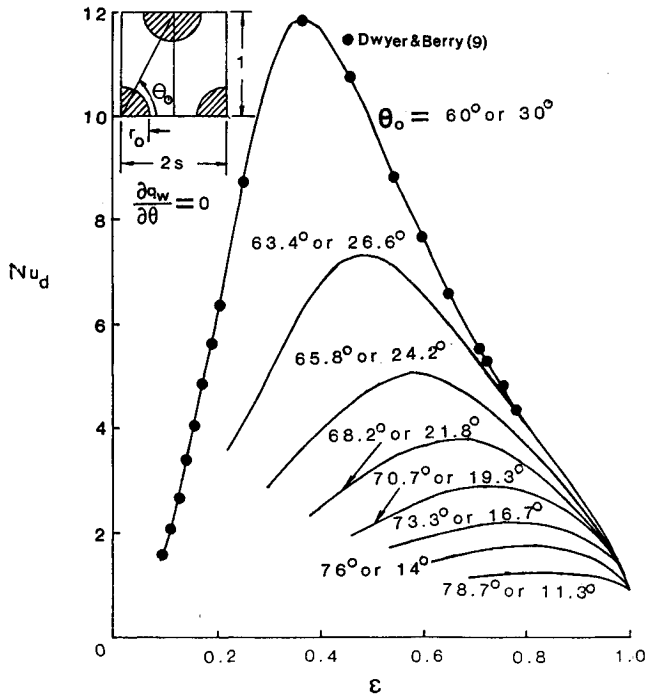

Fig. 3a Nusselt number vs porosity for isosceles triangular arrays at a uniform wall heat flux with 60 deg $\leq \theta_0 \leq$ 90 deg and 0 deg $\leq \theta_0 \leq$ 30 deg.

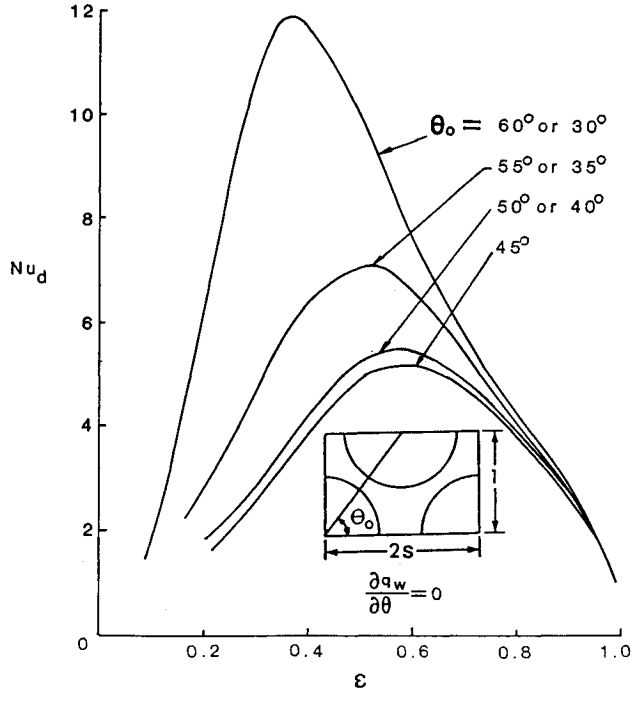

Fig. 3b Nusselt number vs porosity for isosceles triangular arrays at a uniform wall heat flux with 30 deg $\leq \theta_0 \leq$ 60 deg.

Although the theoretical results shown in Figs. 5 and 6 have not been previously published, the limiting case of Fig. 6 with $\theta_0 = 45$ deg (i.e., square array) was investigated by Kim.[15] Unfortunately, numerical errors were found in his Nusselt number calculations. This is observed in Table 2. The results in Table 2 were further double-checked by a finite-element solution.[19] At $s/\bar{r}_0 = 1.1$, Kim overpredicted the Nusselt number Nu_d by 75%. Furthermore, the Nusselt number predicted from his paper and the present work shows a completely different trend, as is seen in Fig. 6.

Numerical computations reveal that the Nusselt number based on the hydraulic diameter exhibits a completely different trend from those based on the actual tube diameter. Both Figs. 7a and 7b illustrate this point. The major difference between Figs. 3 and 7 is that all curves in the latter increase monotonically as the porosity increases. However, the relationship between Nu_d and Nu_{dh} is observed from

$$Nu_{dh} = Nu_d \left[\frac{2}{\pi} \left(\frac{S}{\bar{r}_0} \right)^2 \cot\theta_0 \delta - 1 \right]$$

where δ is defined in the nomenclature.

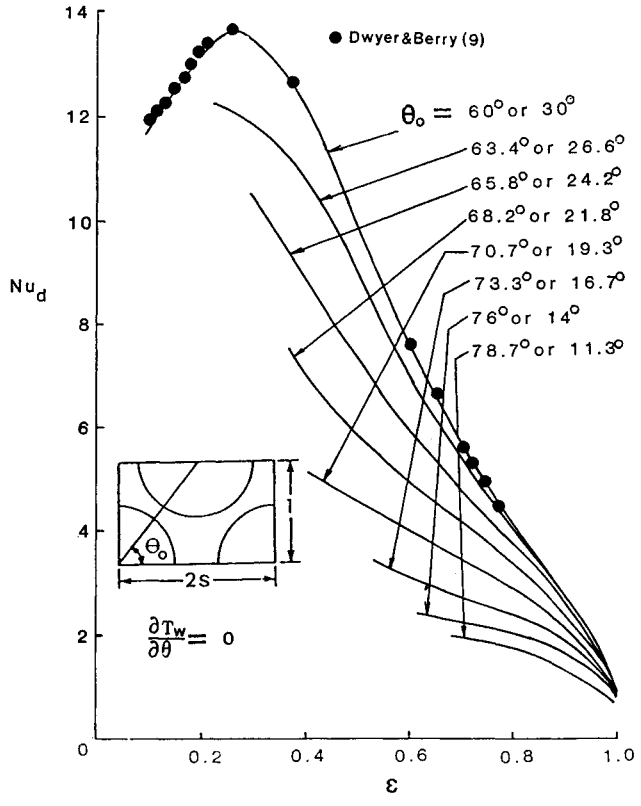

Fig. 4a Nusselt number vs porosity for isosceles triangular arrays at circumferentially uniform temperature with 60 deg $\leq \theta_0 \leq$ 90 deg and 0 deg $\leq \theta_0 \leq$ 30 deg.

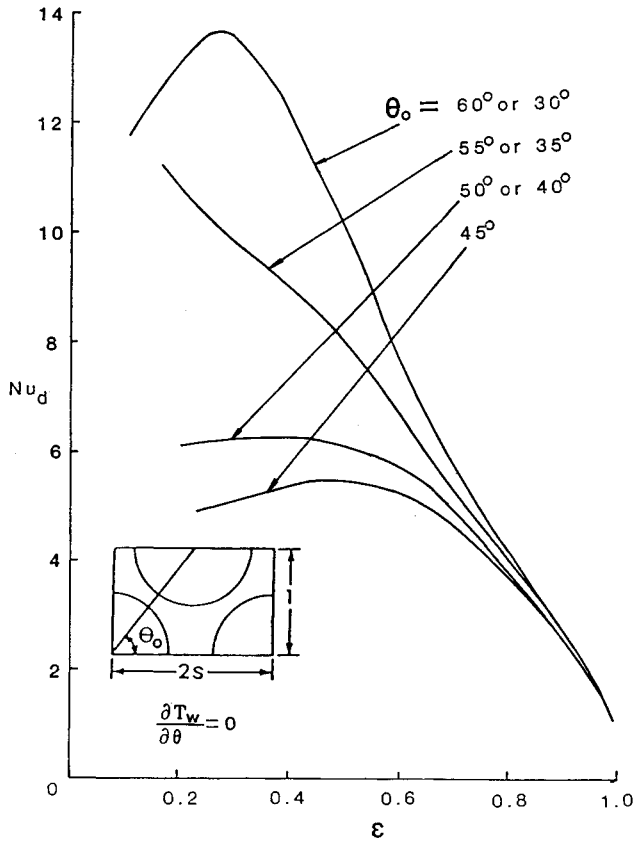

Fig. 4b Nusselt number vs porosity for isosceles triangular arrays with $\partial T_W/\partial\theta = 0$ and 30 deg $\leq \theta_0 \leq$ 60 deg.

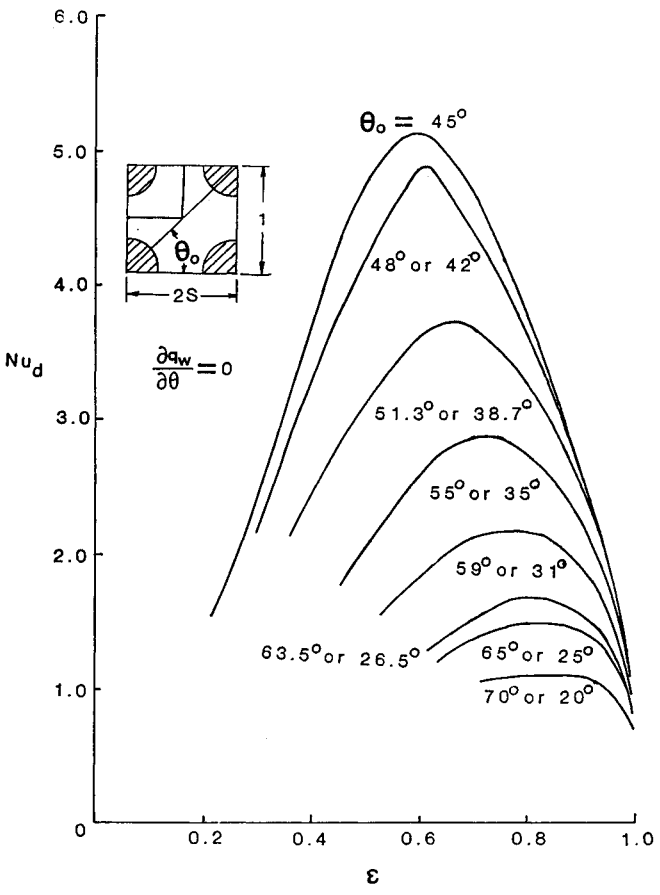

Fig. 5 Nusselt number vs porosity for rectangular arrays with 0 deg $\leq \theta_0 \leq$ 90 deg and $\partial q_W/\partial\theta = 0$.

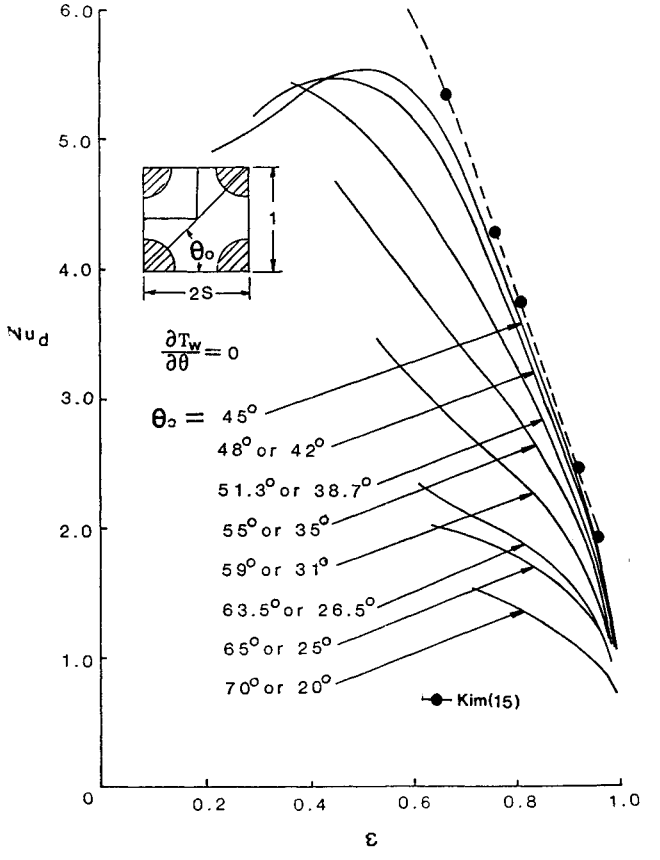

Fig. 6 Nusselt number vs porosity for rectangular arrays with 0 deg $\leq \theta_0 \leq$ 90 deg and $\partial T_W/\partial\theta = 0$.

Table 2 Nusselt numbers Nu_{dh} and Nu_d for square arrays ($\theta_0 = 45$ deg) as functions of $s/\bar{r}_0$ and circumferential boundary conditions

	Uniform wall temperature (H1)			Uniform wall heat flux (H2)	
	Present work		Ref. 15	Present work	
$s/\bar{r}_0$	Nu_{dh}	Nu_d	Nu_d	Nu_{dh}	ϵ
1	1.338	4.895		0.4069	0.2146
1.001	1.351	4.898		0.4116	0.2162
1.01	1.471	4.923		0.4756	0.2301
1.02	1.608	4.953		0.5705	0.2451
1.03	1.749	4.985		0.6781	0.2597
1.04	1.893	5.018		0.7952	0.2739
1.06	2.191	5.087		1.055	0.3010
1.08	2.502	5.158		1.350	0.3267
1.10	2.827	5.228	9.20	1.677	0.3509
1.20	4.576	5.490	7.30	3.667	0.4546
1.30	6.351	5.514	6.48	5.796	0.5353
1.40	7.980	5.336		7.679	0.5993
1.50	9.420	5.052	5.38	9.262	0.6509
1.60	10.703	4.737		10.618	0.6932
1.80	12.965	4.148	4.25	12.939	0.7576
2.0	15.027	3.672	3.73	15.018	0.8037
3.0	25.190	2.408	2.42	25.190	0.9127
4.0	36.589	1.889	1.89	36.539	0.9509
5.0	49.500	1.606		49.500	0.9686
10.0	135.72	1.074		135.72	0.9921

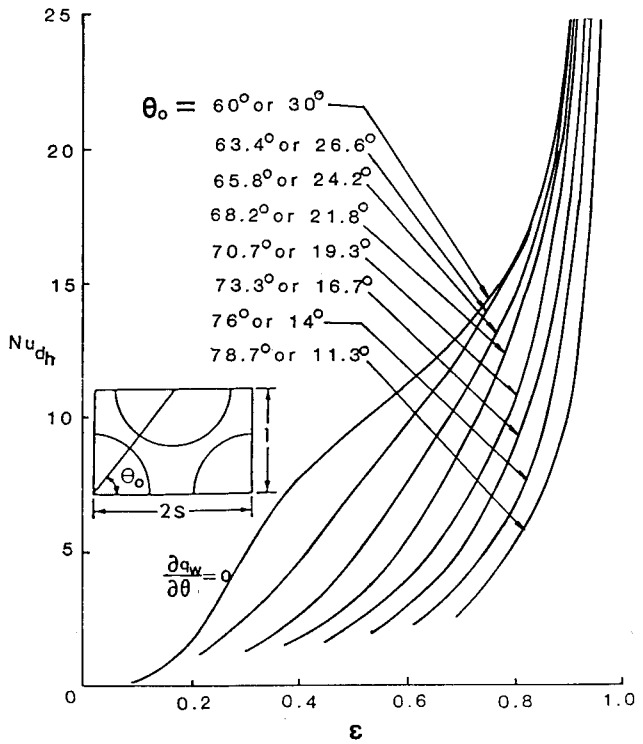

Fig. 7a Nusselt number based on hydraulic diameter vs porosity for isosceles triangular arrays with 60 deg $\leq \theta_0 \leq$ 90 deg and 0 deg $\leq \theta_0 \leq$ 30 deg.

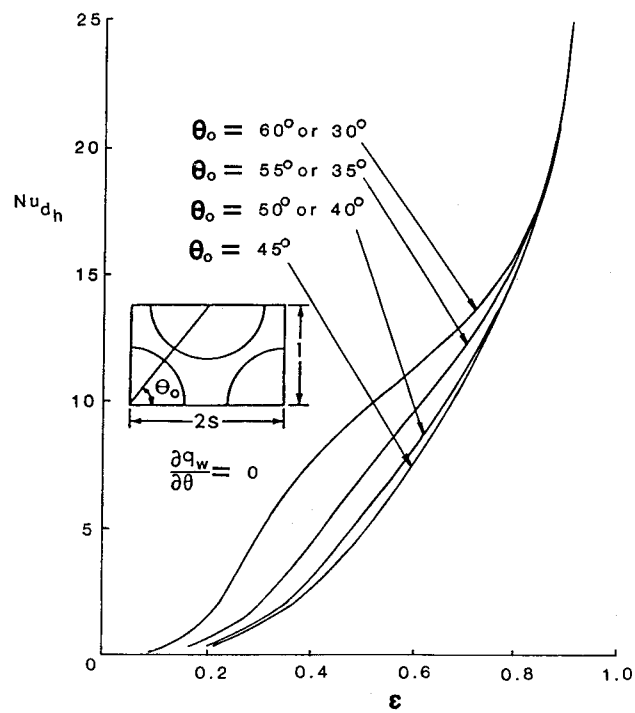

Fig. 7b Nusselt number based on hydraulic diameter vs porosity for isosceles triangular arrays with 30 deg $\leq \theta_0 \leq$ 60 deg.

The term inside the bracket is very sensitive to ϵ and becomes a dominant factor as ϵ changes. Consequently, the use of hydraulic diameter in Nusselt number tends to obscure the physics. For this reason, the tube diameter being a characteristic length is preferred in our study, although the hydraulic diameter was employed by many previous investigators.

For rectangular arrays with two pairs of rods in contact, and under the uniform heat flux circumferentially, the hot spot always exists at $\alpha = 0$. The surface temperature drops drastically as α increases, unless θ_0 is near 45 deg. As $\theta_0 = 45$ deg, the surface temperature becomes completely symmetric with respect to $\alpha = 45$ deg. Additional interesting results with rods in point contact are available in Ref. 20. Figure 8 indicates that the surface temperature is also symmetrical; even tubes are not in point contact. The dash line in this figure represents the average value of each curve. As is expected, the wall temperature becomes more uniform along angular direction when $s/\bar{r}_0$ is large.

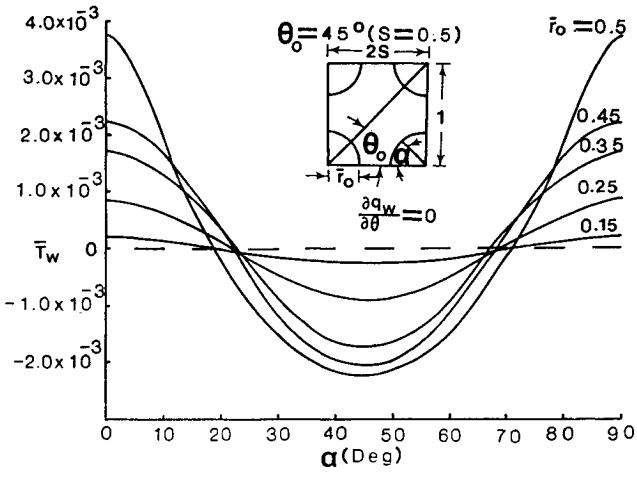

Fig. 8 Dimensionless local wall temperature for a square array ($\theta_0 = 45$ deg) with various rod sizes subjected to a uniform wall heat flux.

A unique feature of the present work is the use of porosity as an independent variable instead of $s/\bar{r}_0$, although the latter was widely used in the literature. In the present problem, the use of ϵ is more convenient and compact than $s/\bar{r}_0$ in graphical presentation for the following reasons: 1) For any physical system, the variable $s/\bar{r}_0$ ranges from 1 to infinity, whereas ϵ ranges only from 0 to 1; 2) when Nu_d (not Nu_{dh}) is plotted against ϵ, the curve with $\theta_0 = 45$ deg or $\theta_0 = 60$ deg can be treated as an asymptotic curve as ϵ approaches unity. Nevertheless, the conversion between porosity and pitch to diameter ratio can be easily made from the following simple relation:

$$\epsilon = 1 - \frac{\pi}{2}\delta \cot\theta_0/(s/\bar{r}_0)^2$$

Conclusion

Temperature distribution of the flow through isosceles triangular and rectangular arrays of rod bundles is solved using the collocation method. Based on this result, the average Nusselt number, local wall heat transfer rate, and local wall temperature distribution are determined. Two limiting solutions of Nusselt number with $\theta_0 = 60$ deg and $\theta_0 = 45$ deg (equilateral triangular and square arrays) were examined. The former agrees well with Dwyer and Berry[9] for all values of ϵ, whereas the latter agrees with Kim[15] only when $\epsilon > 0.6$.

Acknowledgment

The support of Texas Instruments Inc. under a research grant is gratefully acknowledged.

References

[1]Miller, P., Byrnes, J. J., and Benforado, D. M., "Heat Transfer to Water Flowing Parallel to a Rod Bundle," *American Institute of Chemical Engineering Journal,* Vol. 2, 1956, pp. 226-234.

[2]Parrette, J. R. and Grimble, R. E., "Average and Local Heat Transfer Coefficients for Parallel Flow Through a Rod Bundle," Westinghouse Electric Corp., Pittsburgh, PA, WAPD-TH 180, March 1956.

[3]Palmer, L. K. and Swenson, L. L., "Measurements of Heat Transfer Coefficients, Friction Factor, and Velocity Profiles for Air Flowing Parallel to Closely Spaced Rods," *International Developments in Heat Transfer,* Vol. 3, No. 63, 1961, pp. 535-542.

[4]Wantland, J. L., "Compact Tubular Heat Exchangers," Reactor Heat Transfer Conference of 1956, NY, TID-7529, Pt. 1, Book 2, 1956, p. 525.

[5]Rogers, J. T., Chapman, T. M., and Barns, G. M., "Local Heat Transfer Coefficients in Simulated Reactor Fuel Element Bundles," paper presented at the Regional Technical Conference on Heat Transfer, Kingston, Canada, 1964.

[6]Marek, J. and Rehme, K., "Heat Transfer in Smooth and Roughened Rod Bundles Near Spacer Grids," *Fluid Flow and Heat Transfer Over Rod or Tube Bundles,* edited by S. C. Yao and P. A. Pfund, ASME, NY, 1979, pp. 163-170.

[7]Han, J. T., "Heat Transfer in a Partially Blocked Sodium-Coal and Rod Bundle," *Fluid Flow and Heat Transfer Over Rod or Tube Bundles,* edited by S. C. Yao and P. A. Pfund, ASME, NY, 1979, pp. 187-191.

[8]Sparrow, E. M., Loeffler, A. L., and Hubbard, H. A., "Heat Transfer to Longitudinal Laminar Flow Between Cylinders," *Journal of Heat Transfer,* Transactions of ASME, Vol. 83, 1961, pp. 415-422.

[9]Dwyer, O. E. and Berry, H. C., "Laminar-Flow Heat Transfer for In-Line Flow Through Unbaffled Rod Bundles," *Nuclear Science and Design,* Vol. 42, 1970, pp. 81-88.

[10]Dwyer, O. E. and Tu, P. S., "Heat Transfer Rates for Parallel Flow of Liquid Metals Through Tube Bundles—I," American Institute of Chemical Engineering, Paper 119, 3rd National Heat Transfer Conference, Storrs, CT, 1959.

[11]Friedland, A. J. and Bonilla, C. F., "Analytical Study of Heat Transfer Rates for Parallel Flow of Liquid Metals Through Tube Bundles—II," *American Institute of Chemical Engineering Journal,* Vol. 7, Jan. 1961, pp. 107-122.

[12]Axford, R. A., "Two Dimensional Multiregion Analysis of Temperature Fields in Reactor Tube Bundles," *Nuclear Engineering Design,* Vol. 6, Aug. 1967, pp. 25-42.

[13]Graber, H., "Heat Transfer in Smooth Tubes, Between Parallel Plates in Annuli and Tube Bundles with Exponential Heat Flux Distributions in Forced Laminar or Turbulent Flow," *International Journal of Heat Mass Transfer,* Vol. 13, Nov. 1970, pp. 1645-1703.

[14]Yang, J. W., "Heat Transfer and Fluid Flow in Regular Rod Arrays with Opposing Flow," *Fluid Flow and Heat Transfer Over Rod or Tube Bundles,* edited by S. C. Yao and P. A. Pfund, ASME, NY, 1979, pp. 149-153.

[15]Kim, J. H., "Heat Transfer in Longitudinal Laminar Flow Along Circular Cylinders in Square Array," *Fluid Flow and Heat Transfer Over Rod or Tube Bundles,* edited by S. C. Yao and P. A. Pfund, ASME, NY, 1979, pp. 155-161.

[16]Axford, R. A., "Summary of Theoretical Aspects of Heat Transfer Performance in Clustered Rod Geometries," *Heat Transfer in Rod Bundles,* ASME, 1968, pp. 70-103.

[17]Shah, R. K. and London, A. L., "Laminar Flow Forced Convection in Ducts," *Advances in Heat Transfer,* Supp. I, Academic Press, NY, 1978.

[18]Chung, B. T. F., Liu, F., Kermani, M. M., and Yeh, L. T., "Longitudinal Laminar Flow Through Isosceles Triangular and Rectangular Rod Bundles," *Advances in Heat Exchanger Design,* Vol. 66, edited by R. Shah and J. Pearson, Heat Transfer Division, 1986, pp. 45-53.

[19]Chung, B. T. F., Kermani, M. M., and Liu, F., "Heat and Momentum Transfer from a Solid State Phased Array Radar," TR, Department of Mechanical Engineering, Univ. of Akron, 1986.

[20]Chung, B. T. F., Liu, F., Kermani, M. M., and Yeh, L. T., "Heat Transfer from Parallel Flow Through Isosceles Triangular and Rectangular Tube Bundles," AIAA Paper 87-0079, presented at AIAA 25th Aerospace Sciences Meeting, Reno, NV, 1987.